Received: 25 March 2024 | Accepted: 13 August 2024

DOI: 10.1002/hem3.70024

ARTICLE

HemaSphere EHA EUROPEAN HEMATOLOGY ASSOCIATION

Testicular large B-cell lymphoma is genetically similar to PCNSL and distinct from nodal DLBCL

Alfredo Rivas-Delgado[1,2,3,^] | Cristina López[2,4,5,^] | Guillem Clot[2,4] | Ferran Nadeu[2,4] | Marta Grau[2,4] | Gerard Frigola[6] | Jan Bosch-Schips[7] | Josefine Radke[8,9] | Naveed Ishaque[10] | Miguel Alcoceba[3,4,11,12] | Gustavo Tapia[13,14] | Luis Luizaga[15] | Carmen Barcena[16] | Nicholas Kelleher[3,17] | Neus Villamor[2,4,6] | Tycho Baumann[3,16] | Ana Muntañola[3,15] | Juan M. Sancho-Cia[3,13] | Alejandro M. García-Sancho[3,4,11,12] | Eva Gonzalez-Barca[3,5,18] | Estella Matutes[6] | Jordi A. Brito[19] | Kennosuke Karube[20] | Itziar Salaverria[2,4] | Anna Enjuanes[2,4] | Stefan Wiemann[21,22] | Frank L. Heppner[8,22] | Reiner Siebert[23] | Fina Climent[3,7] | Elías Campo[2,4,5,6] | Eva Giné[1,2,3,4] | Armando López-Guillermo[1,2,3,4,24,^] | Silvia Beà[2,3,4,5,6,^]

Correspondence: Cristina López (clopez2@clinic.cat)

Abstract

Testicular large B-cell lymphoma (TLBCL) is an infrequent and aggressive lymphoma arising in an immune-privileged site and has recently been recognized as a distinct entity from diffuse large B-cell lymphoma (DLBCL). We describe the genetic features of TLBCL and compare them with published series of nodal DLBCL and primary large B-cell lymphomas of the CNS (PCNSL). We collected 61 patients with TLBCL. We performed targeted next-generation sequencing, copy number arrays, and fluorescent *in situ* hybridization to assess chromosomal rearrangements in 40 cases with available material. Seventy percent of the cases showed localized stages. *BCL6* rearrangements were detected in 36% of cases, and no concomitant *BCL2* and *MYC* rearrangements were found. TLBCL had fewer copy number alterations ($p < 0.04$) but more somatic variants ($p < 0.02$) than nodal DLBCL and had more frequent 18q21.32-q23 (*BCL2*) gains and 6q and 9p21.3 (*CDKN2A/B*) deletions. *PIM1*, *MYD88*^{L265P}, *CD79B*, *TBL1XR1*, *MEF2B*, *CIITA*, *EP300*, and *ETV6* mutations were more frequent in TLBCL, and *BCL10* mutations in nodal DLBCL. There were no major genetic differences between TLBCL and PCNSL. Localized or disseminated TLBCL displayed similar genomic profiles. Using LymphGen, the majority of cases were classified as MCD. However, we observed a subgroup of patients classified as BN2, both in localized and disseminated TLBCL, suggesting a degree of genetic heterogeneity in the TLBCL genetic profile. TLBCL has a distinctive genetic profile similar to PCNSL, supporting its recognition as a separate entity from DLBCL and might provide information to devise targeted therapeutic approaches.

[1]Department of Hematology, Hospital Clínic, Barcelona, Spain
[2]Institut d'Investigacions Biomèdiques August Pi i Sunyer (IDIBAPS), Barcelona, Spain
[3]Grupo Español de Linfomas y Trasplante de Médula Ósea (GELTAMO), Madrid, Spain
[4]Centro de Investigación Biomédica en Red de Cáncer (CIBERONC), Madrid, Spain
[5]Departament de Fonaments Clínics, Universitat de Barcelona, Barcelona, Spain
[6]Department of Pathology, Hospital Clínic, Hematopathology Section, Barcelona, Spain
[7]Department of Pathology, Hospital Universitari de Bellvitge, IDIBELL, Hospitalet de Llobregat, Spain

INTRODUCTION

Testicular lymphoma is a rare and aggressive lymphoma accounting for 1%–2% of all non-Hodgkin's lymphomas (NHL) and 4% of extranodal lymphomas.[1,2] Approximately 80%–90% of testicular lymphomas correspond to diffuse large B-cell lymphoma (DLBCL).[3] The 5th edition of the World Health Organization (WHO) classification defines a new entity, "Primary large B-cell lymphoma of immune-privileged sites," encompassing primary large B-cell lymphoma of the CNS, vitreoretinal compartment, and testes.[4] The International Consensus Classification of Mature Lymphoid Neoplasms recognizes primary DLBCL of the testis as a separate entity, but it remains uncertain whether extranodal lymphomas arising in immune-privileged sites should be grouped as a unique entity.[5] The majority of testicular large B-cell lymphoma (TLBCL) patients present with localized stages (stage I–II), although 20%–30% of the cases may exhibit disseminated disease.[6] TLBCL has marked extranodal tropism, being the central nervous system (CNS) and contralateral testis as the most common sites of dissemination.[7,8] Although the outcome of TLBCL patients substantially improved after the introduction of rituximab, they still show frequent relapses or treatment failure and, therefore, a poor prognosis.[8,9]

Around 70%–90% of TLBCLs resemble the activated B-cell (ABC) or nongerminal center subtype of nodal DLBCL,[10–12] and the majority of cases cluster among the recently described molecular subgroups MCD/C5, with frequent genetic alterations of NF-κB, Toll-like receptor (TLR), and B-cell receptor (BCR) signaling pathways, including somatic mutations of *MYD88*^{L265P}, *CARD11*, and *CD79B*.[13–15] TLBCL develops in an immune-privileged site behind the blood-testis barrier and shares some genetic alterations with primary large B-cell lymphomas of the CNS (PCNSL), including the mutations described above, *CDKN2A* (9p21) mutation/loss, structural rearrangements in the *PD-1/PD-2* loci (9p24), and frequent loss of HLA class I and II expression or loss of HLA loci (6p21), leading to immune evasion.[16,17]

The genetic alterations in TLBCL, including the similarities with PCNSL and differences from nodal DLBCL, have not been fully characterized. Herein, we investigated the genomic profile of TLBCL, looking at the clinical impact of the genetic lesions in the immunotherapy era, and compared the results with previously published series of PCNSL and nodal DLBCL.

MATERIALS AND METHODS

Patients and samples

We included 61 patients diagnosed with TLBCL according to the updated 4th edition of the WHO[18] classification between 2005 and 2021 in seven institutions from the Spanish group of lymphomas (GELTAMO). The staging was performed according to standard procedures, including PET/CT, unilateral bone marrow biopsy, and lumbar puncture for cerebrospinal fluid analysis by cytology and flow cytometry.[19] We considered localized disease in those cases in Stage I or Stage II with only locoregional lymph nodes involved; all the remaining cases were considered as disseminated. Patients provided written informed consent in accordance with the Declaration of Helsinki, and the study was approved by the Institution's Review Board (HCB/2020/0787). The main clinical-biological features, response to therapy, and outcome were recorded and analyzed. All but five patients were treated with chemoimmunotherapy, followed by radiotherapy to the contralateral testis in 62% of the patients (Table 1). Responses were assessed by end-of-therapy PET/CT according to standard guidelines.[20]

Two independent series were used to compare the genetic features of TLBCL: (i) 112 patients with nodal DLBCL from our institution[21] and (ii) 39 PCNSL patients previously published.[22]

Histological review

Histological diagnosis, including morphology and immunohistochemistry, was reviewed by expert pathologists. *MYC*, *BCL2*, *BCL6*, *JAK2*, and *IRF4* rearrangements were assessed by Fluorescence *in situ* hybridization (FISH) using break-apart and/or dual-color dual-fusion commercial probes (Metasystems) (Supporting Information S1: Materials and Methods). HLA class I (HLA-A) and II (HLA-DR) expression were determined by immunohistochemistry (Supporting Information S1: Table 1 and Supporting Information S1: Materials and Methods). Cell-of-origin (COO) assessment was performed by immunohistochemistry (IHC) according to the Hans' algorithm and, in the cases with available RNA, through the Lymph2Cx Assay (NanoString Technologies) (Supporting Information S1: Supplementary Materials and Methods).

Copy number alterations (CNA) and targeted next-generation sequencing analysis

DNA and RNA were isolated from 42 formalin-fixed paraffin-embedded (FFPE) and one fresh frozen tissue from diagnostic samples using the AllPrep DNA/RNA FFPE Kit (Qiagen) and QIAmp DNA/RNA Mini Kit (Qiagen), respectively. CNA were analyzed in 42 samples using the Oncoscan CNV FFPE assay and in 1 sample using CytoScan® HD assay (Thermo Fisher Scientific) (Supporting Information S1: Table 2). Nexus version 9.0 Discovery Edition software (Biodiscovery) was used to analyze and visualize results. The human reference genome used

[8]Department of Neuropathology, Charité-Universitätsmedizin Berlin, corporate member of Freie Universität Berlin, Humboldt-Universität zu Berlin, Berlin Institute of Health, Berlin, Germany
[9]Institute of Pathology, Universitätsmedizin Greifswald, Greifswald, Germany
[10]Berlin Institute of Health (BIH) at Charité, Universitätsmedizin Berlin, Center for Digital Health, Berlin, Germany
[11]Department of Hematology, Hospital Universitario de Salamanca, IBSAL, Salamanca, Spain
[12]Department of Hematology, Centro de Investigación del Cáncer-IBMCC (USAL-CSIC), Salamanca, Spain
[13]Departments of Hematology and Pathology, Institut Català d'Oncologia, Hospital Universitari Germans Trias i Pujol, Badalona, Spain
[14]Departament de Ciències Morfològiques, Universitat Autònoma de Barcelona, Barcelona, Spain
[15]Departments of Hematology and Pathology, Hospital Universitari Mutua de Terrassa, Terrassa, Spain
[16]Departments of Hematology and Pathology, Hospital Universitario 12 de Octubre, Madrid, Spain
[17]Department of Hematology, Institut Català d'Oncologia-Hospital Universitari de Girona Doctor Josep Trueta, Girona, Spain
[18]Department of Hematology, Institut Català d'Oncologia-Hospital Duran i Reynals, Hospitalet de Lobregat, IDIBELL, Spain
[19]Department of Surgery, Hospital Clínic, Barcelona, Spain
[20]Department of Pathology and Laboratory Medicine, Nagoya University Hospital, Nagoya, Japan
[21]Division of Molecular Genome Analysis, German Cancer Research Center (DKFZ), Heidelberg, Germany
[22]German Cancer Consortium (DKTK), Partner Site Charité Berlin, Berlin, Germany
[23]Institute of Human Genetics, Ulm University & Ulm University Medical Center, Ulm, Germany
[24]Departament de Medicina, Universitat de Barcelona, Barcelona, Spain
^Alfredo Rivas-Delgado and Cristina López contributed equally as co-first authors; Armando López-Guillermo and Silvia Beà contributed equally as co-senior authors to this work.

TABLE 1 Main baseline features, treatment, and response of the 61 patients with TLBCL.

Characteristics	N (%)
Median age (range)	70 (30–89)
ECOG-PS ≥2	6/48 (12)
B symptoms	6/55 (11)
LDH >UNL	19/50 (38)
Bone marrow infiltration	4/59 (7)
CNS involvement	6/60 (10)
Stage	
I	30 (49)
II	13 (21)
IV	18 (30)
COO Hans' algorithm	
Germinal center B-cell	9/53 (17)
Nongerminal center B-cell	44/53 (83)
COO LymphC2x	
Germinal center B-cell	7/42 (17)
Activated B-cell	30/42 (71)
Unclassified	5/42 (12)
FISH	
MYC rearrangement	4/50 (8)
BCL2 rearrangement	2/45 (4)
BCL6 rearrangement	17/47 (36)
IPI	
Low risk	27/49 (55)
Low-Intermediate risk	9/49 (18)
High-Intermediate risk	3/49 (6)
High risk	10/49 (21)
HLA loss	
HLA class I	37/41 (91)
HLA class II	28/43 (62)
Treatment	
R-CHOP	47 (77)
Intensive chemoimmunotherapy	5 (8)
R-CVP	4 (7)
Died before starting treatment or palliative care	5 (8)
Response to treatment	
Complete response	45/56 (80)
Partial response	1/56 (2)
Progressive disease	10/56 (18)

Note: Intensive chemoimmunotherapy includes BURKIMAB (rituximab, methotrexate, ifosfamide, vincristine, etoposide, cytarabine, cyclophosphamide, doxorubicin, vindesine, and dexamethasone) and Hyper-CVAD (cyclophosphamide, vincristine, doxorubicin, methotrexate, cytarabine, and dexamethasone).

Abbreviations: CNS, Central nervous system; COO, cell-of-origin; ECOG-PS, Eastern Cooperative Oncology Group performing status; FISH, fluorescence *in situ* hybridization; IPI, International Prognostic Index; R-CHOP, rituximab, cyclophosphamide, doxorubicin, vincristine, prednisone; R-CVP, rituximab, cyclophosphamide, vincristine, and prednisone; UNL, upper normal limit.

was GRCh37/hg19. Driver CNAs were determined by the GISTIC algorithm (2.0.23).[23]

Single nucleotide variants (SNVs) and short insertions/deletions (indels) were evaluated in 42 samples using a B-cell malignancy-oriented targeted panel covering 115 genes (SureSelectXT; Agilent Technologies) (Supporting Information S1: Table 3 and Supporting Information S1: Methods) and sequenced in a MiSeq instrument (Illumina). The bioinformatic analysis was performed using an updated version of our in-house pipeline[24,25] (Supporting Information S1: Methods). The LymphGen 2.0 probabilistic classification tool was used to classify TLBCL cases into the recently described genetic subtypes.[13]

Statistical analysis

Fisher's exact test was used to evaluate the association between categorical variables. Negative binomial generalized linear models, implemented in the *glm.nb* function of the MASS R package, were used to evaluate the associations between the accumulation of alterations and the lymphoma entities, adjusting for the COO. An exact conditional test implemented in the *mantelhaen.test* R function was used to evaluate the association between the presence of an alteration and the lymphoma entity, adjusting for the COO. The endpoints were progression-free survival (PFS) and overall survival (OS). The log-rank test or Cox regression was used to evaluate the association between the endpoints and categorical or quantitative variables, respectively. Cox regression was also used to estimate the hazard ratios (HR). *p*-Values were adjusted using the Benjamini-Hochberg method. To reduce the potential bias created by the detection sensibility of mutations and CNAs by the different technologies used in the TLBCL and PCNSL series, when comparing those series, TLBCL mutations with VAF < 10% and PCNSL CNA segments smaller than 100 kb were filtered out. The Non-negative Matrix Factorization method solved with the brunet algorithm, implemented in the NMF R package, was used to perform an unsupervised cluster analysis of the cases from the TLBCL, DLBCL, and PCNSL series.[26] The input variables were the presence/absence of alterations in the driver CNAs and in the panel genes available in the three series. Genes/regions with less than five alterations were filtered out in this analysis, as well as cases with missing information in any of the input variables. Two stable clusters were identified according to the cophenetic metric.

RESULTS

Baseline features

The main clinical-biological characteristics of the patients are listed in Table 1. The median age was 70 years and 30% of the patients had disseminated disease at diagnosis, including 6 cases with CNS involvement (Supporting Information S1: Table 2). A high prevalence of loss of HLA class I (37/41, 91%) and HLA class II (28/43, 62%) expression was observed (Supporting Information S1: Figure 1). To determine the COO by Hans' algorithm, immunohistochemical evaluation of CD10, BCL6, and MUM1 was available in 53 cases, of which 44 (83%) were categorized as non-GCB subtype, and 9 were classified as GCB subtype. Among the nine GCB cases, eight of them had an ambiguous phenotype with co-expression of CD10 and MUM1. Lymph2Cx assay classified 42 cases into three categories: 71% ABC, 17% GCB, and 12% unclassified. The concordance rate between the Lymph2Cx assay and Hans' algorithm was 76% (Supporting Information S1: Figure 2). Three of the eight patients with

ambiguous immunophenotypes by Hans' algorithm were classified as ABC and one remained unclassified by Lymph2Cx. Of note, in any of these cases, neither plasmablastic morphology nor *IRF4* rearrangement (available in 4 out of 8) was observed (Supporting Information S1: Table 2). On the other hand, *MYC*, *BCL2*, and *BCL6* rearrangements were found in 8%, 4%, and 36% of cases, respectively. Two cases showed simultaneous *MYC* and *BCL6* rearrangement, while no concomitant *BCL2* and *MYC* rearrangement were detected. Double-expressor phenotype was observed in 39% of the cases ($N = 11/28$).

Copy number profiling

To determine the recurrent chromosomal abnormalities, including CNA and copy number neutral loss of heterozygosity (CN-LOH), we performed SNP arrays on 43 cases. Our analysis revealed a median of 13 CNAs per case (range 1–43), comprising 6 gains (range 0–24), 6 losses (range 0–28), and 2 CN-LOH per case (range 0–10) (Supporting Information S1: Table 4). The most frequently observed CNA regions (>10%) were: (i) gains 19q13 (*SPIB*), 1q, 18q21-q22 (*BCL2*), 6p25-p22, 9p13 (*ZCCHC7*), 4q, 11q24-q25 (*ETS1*, *FLI1*), 9p24 (*JAK2*), and 17q12-q21; (ii) trisomies 18, 3, 7, 12, and 21; and (iii) losses of 9p21 (*CDKN2A/B*), 6q21 (*PRDM1*), 6q23-q24 (*TNFAIP3*), 1q32-q44, 15q15 (*B2M*), 17p13 (*TP53*), 6p21 (*HLA-C*, *HLA-B*), 1p35, 14q32 (*BCL11B*, *EVL*), and 1p36, and CN-LOH 9p, 6p25-p23, 3p, and 3q (Figure 1). We also observed homozygous deletions at 9p21 (*CDKN2A/B*) and high copy gains at 18q21.31-q23 (*BCL2*) in 51% (22/43) and 9% (4/43) of the cases, respectively. Using GISTIC, we identified five driver CNA ($q < 0.05$): losses of 1p35, 6p21 (*HLA-C*, *HLA-B*), 6q21 (*PRDM1*), 9p21 (*CDKN2A/B*), and 1q gains (Supporting Information S1: Table 5). The 9p24.1 genomic region has been previously described as frequently altered in TLBCL;[16] we identified seven cases (16%) with genomic alterations in this region, including four gains detected by arrays and two gains and one break detected by FISH using a *JAK2* probe. Chromothripsis was observed in 12 (28%) cases, involving frequently (≥2 cases) chromosomes 1, 6, and 7 (Supporting Information S1: Figure 3). Notably, 58% (7/12) of these cases harbored genomic alterations (mutations or deletions) in *TP53*, *ATM*, or *SETD2* loci, previously associated with genomic instability and chromothripsis.[27–30]

Genomic alterations and integrative analysis

A 115-gene custom-targeted sequencing panel was used to analyze 42 samples. The mean coverage of the samples was 599x (range 32–2001) (Supporting Information S1: Table 6). The median number of mutations per sample was 14 (range 1–132) (Supporting Information S1: Table 7). Integrating CNA, SNV, and indels in the 40 cases with NGS and CNA available, the genes/regions altered in >40% of the cases were *PRDM1* (68%), *CDKN2A/B* (68%), *TNFAIP3* (65%), *SGK1* (62%), *ARID1B* (60%), $MYD88^{L265P}$ (57%), *SPIB* (55%), *PIM1* (55%), *CD79B* (50%), *KMT2D* (48%), *SETD1B* (48%), *OSBPL10* (42%), and gain of 19q13 (52%) and 1q (48%) (Figure 2). Concomitant mutations in $MYD88^{L265P}$, *CD79B*, and *PIM1* were detected in twelve (29%) cases (note that case TLBCL3 only had NGS data available). Seventy-one percent of the cases (30/42) could be classified into a molecular subgroup according to the LymphGen tool, the distribution was as follows: MCD, 20 cases (66%); BN2, 7 cases (24%), EZB, 2 cases (7%); composite (EZB/MCD/ST2), 1 case (3%) (Figure 2).

However, within both the localized and disseminated TLBCL cohorts, we have identified a subset of patients categorized as BN2. Notably, these individuals lacked concurrent alterations in $MYD88^{L265P}$/*PIM1*/*CD79B* (Supporting Information S1: Figure 4) and did not exhibit amplification of 9p24.3-p24.1. Instead, they exclusively manifested biallelic alterations in *TNFAIP3* and *BCL10* mutations. Additionally, they demonstrated a decreased frequency of mutated genes associated with immunoevasion, such as *CD58*, *CIITA*, and loss of 6p21.33. Moreover, we identified that the BN2 group is enriched in the GBC subtype and *BCL6* rearrangement ($p = 0.029$ and $p = 0.006$, respectively; Supporting Information S1: Table 8). In contrast, the MCD group is characterized by the ABC subtype. After correcting for multiple testing, we found that $MYD88^{L265P}$ and *KMT2D* alterations are significantly enriched in the MCD subgroup (adj. $p = 0.007$ and $p = 0.045$, respectively). Collectively, these findings underscore the genetic heterogeneity present within TLBCL.

Localized versus disseminated disease

We compared patients with localized (stages I and II, $N = 43$) versus patients with disseminated disease (stage IV, $N = 18$) since some of the latter might not correspond to primary TLBCL. As expected, patients with systemic disease significantly showed more frequent B symptoms, poorer performance status (ECOG index), higher LDH levels, and higher International Prognostic Index (IPI) scores. No major differences were observed in the COO subtype, LymphGen subgroups, and *MYC*, *BCL2*, or *BCL6* rearrangements (Figure 2 and Supporting Information S1: Table 9). Interestingly, patients with localized or disseminated disease displayed similar genomic complexity based on the number of CNAs and mutated genes (Supporting Information S1: Figure 5). For this reason and to increase the statistical power both clinical groups were considered together and compared with nodal DLBCL and PCNSL series.

TLBCL and PCNSL share genetic alterations that differ from nodal DLBCL

We compared the CNAs and the mutational profile of TLBCL with previously published series of DLBCL[21] (NGS panel and CNA) and PCNSL[22] (whole genome sequencing). For the comparative analyses, only the overlapping genes from both NGS panel designs were considered ($N = 60$). PCNSL copy number profiles were assessed by ACE-seq, and the mutational analysis was made only considering the regions from the 115 genes present in the TLBCL panel. Due to the differences between the methodologies employed for the PCNSL and TLBCL sequencing analyses, only mutations in the TLBCL series with a variant allele frequency (VAF) greater than 10% were considered. To account for the different ABC/GCB frequencies between the three entities, all comparisons were adjusted for the COO (cases without COO information were excluded).

Compared with nodal DLBCL, localized and disseminated TLBCL have less CNA complexity ($p = 0.008$ and $p = 0.039$, respectively) but showed a higher number of mutations ($p = 0.011$ and $p < 0.001$, respectively) and a higher number of mutated genes ($p = 0.027$ and $p < 0.001$, respectively) (Supporting Information S1: Figure 5). TLBCL presented more frequently 18q21.32-q23 (*BCL2*) gains, and 6q and 9p21.3 (*CDKN2A/B*) deletions (Figure 3 and Supporting Information S1: Table 10). In contrast, 2p16.2-p13.3 (*REL* and *BCL11A*) and 8q22.3-q24.3 (*MYC*) gains, trisomy 5, and 1p and 13q14 deletions were more frequently observed in nodal DLBCL. Furthermore, *PIM1*, $MYD88^{L265P}$, *CD79B*, *TBL1XR1*, *MEF2B*, *CIITA*, *EP300*, and *ETV6* mutations were enriched in TLBCL, and *BCL10* mutations in nodal DLBCL (Figure 3 and Supporting Information S1: Table 11). Importantly, biallelic inactivation of *CDKN2A/B* and *PRDM1* was more prevalent in TLBCL compared to nodal DLBCL (Supporting Information S1: Table 12).

No clear differences in the number of mutations or the number of mutated genes were observed between TLBCL and PCNSL

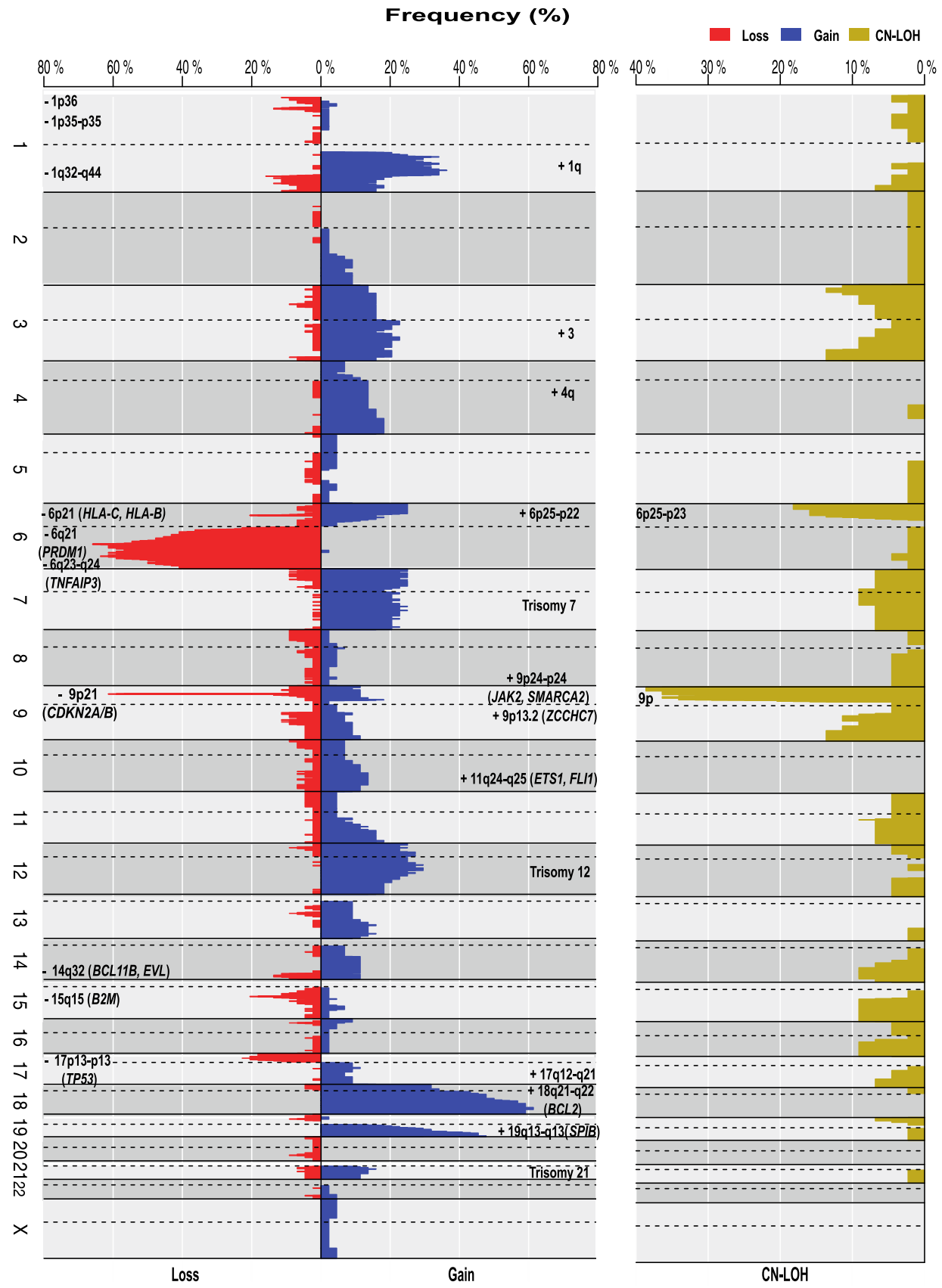

FIGURE 1 **Copy number profile of TLBCL.** Copy number profile (left panel) and copy number loss of heterozygosity (CN-LOH) (right panel) of 43 TLBCL. On the *y*-axis, the chromosomes are represented vertically from 1 to X (chromosome Y is excluded); on the *x*-axis, the percentages of patients with CNA and CN-LOH are shown with gains in blue, losses in red, and CN-LOH in yellow. Regions with CNA and CN-LOH frequency ≥10% and potential target genes are indicated.

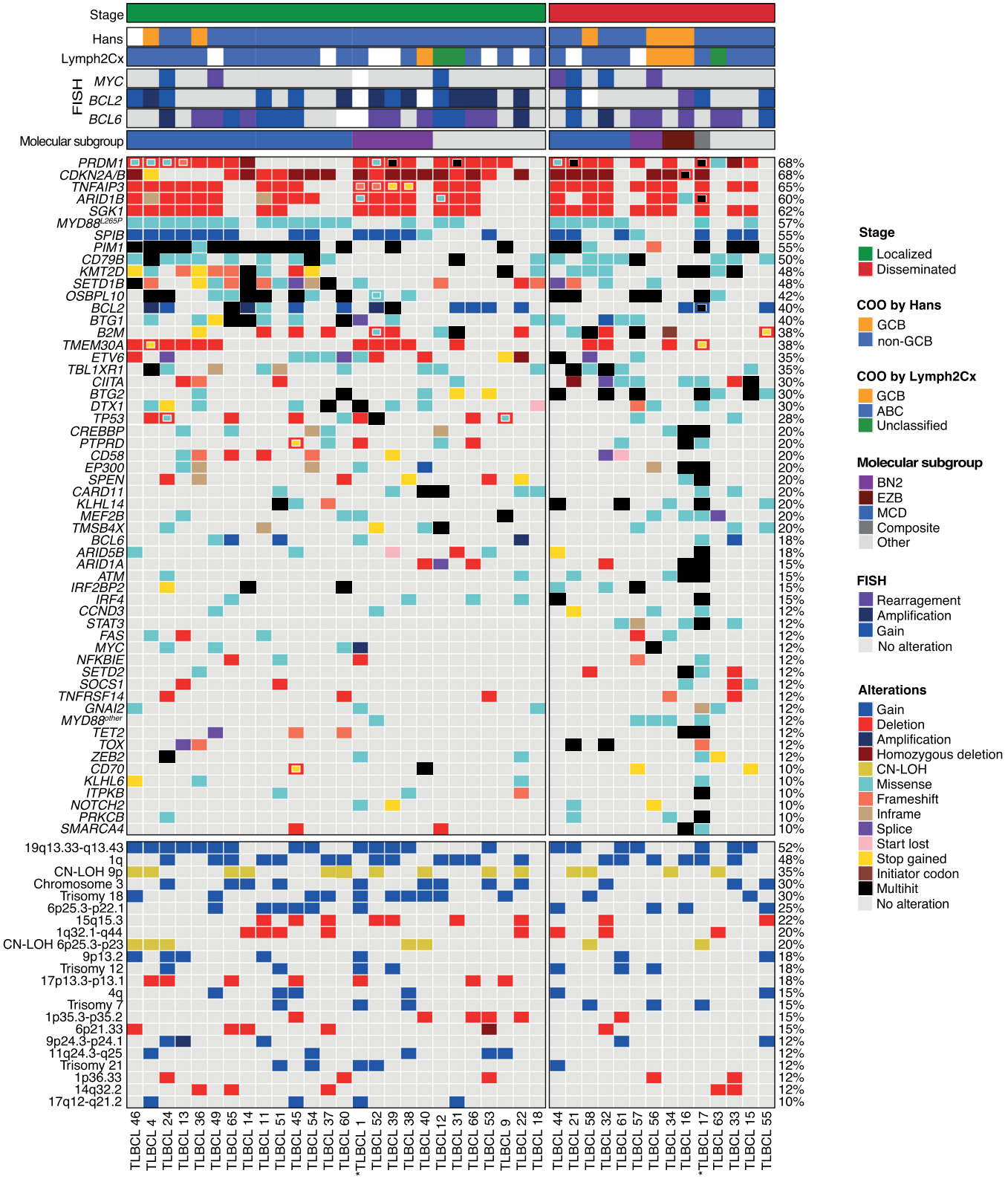

FIGURE 2 **Recurrent genomic alterations in TLBCL according to disease stage.** The Oncoprint encompasses the 40 samples analyzed using next-generation sequencing and copy number analysis. Each column represents one tumor sample, and each row represents one gene/region. Altered genes and genomic regions with a frequency ≥10% are ordered by decreasing frequency. From top to bottom: stage of the disease; COO by Hans' algorithm and Lymph2Cx; *MYC*, *BCL2*, and *BCL6* rearrangements; molecular subgroups according to LymphGen analysis; single nucleotide variants (SNVs), small insertions/deletions (indels), and copy number alterations (CNA). *Low coverage, higher probability of false positives.

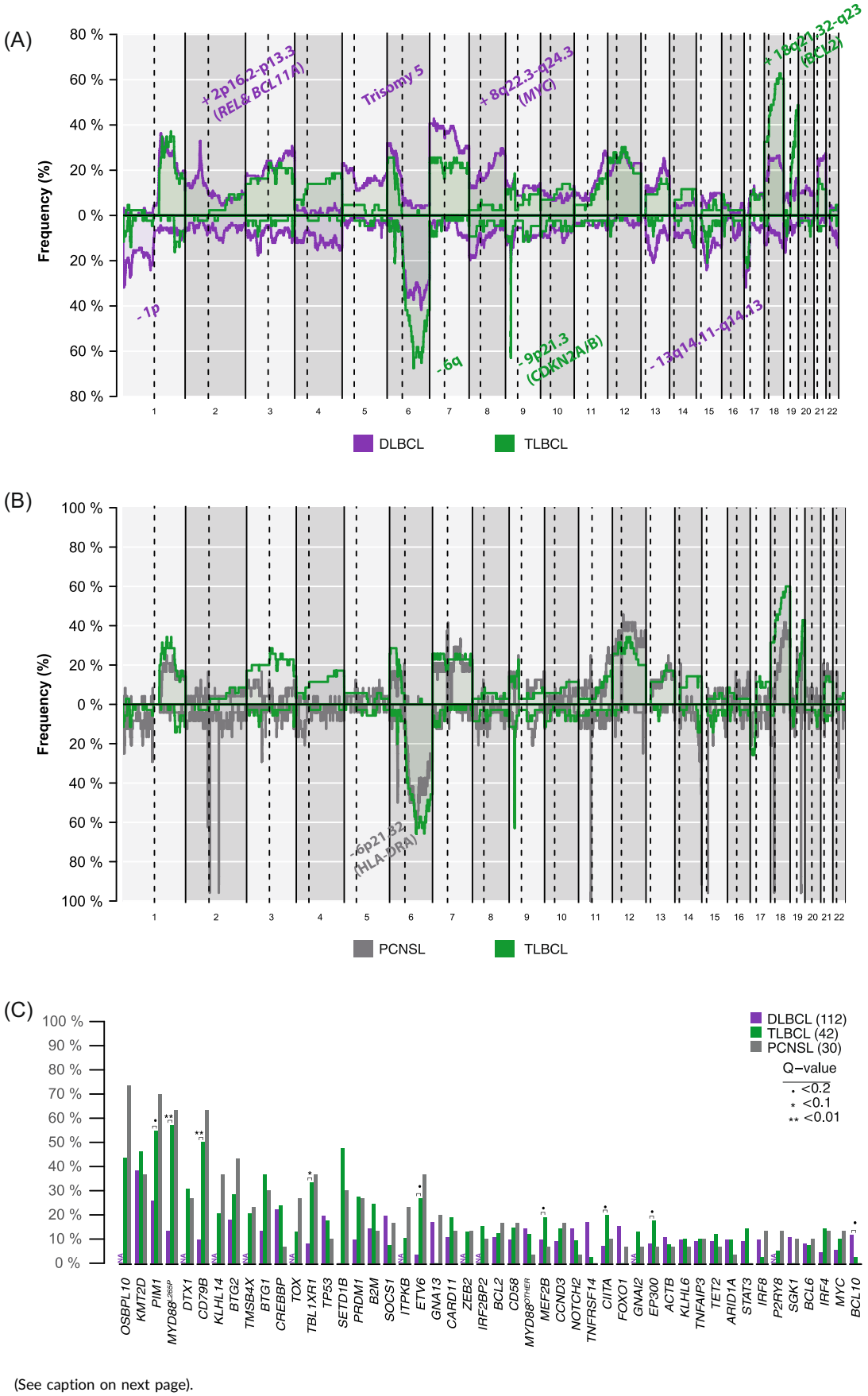

FIGURE 3 (See caption on next page).

FIGURE 3 **Comparison of the copy number alterations (CNA) and mutation frequencies between testicular large B-cell lymphoma (TLBCL), diffuse large B-cell lymphoma (DLBCL), or primary large B-cell lymphomas of the CNS (PCNSL).** **(A)** Comparison of CNA between TLBCL cases and nodal DLBCL, highlighting biologically relevant regions with differential frequency (color denotes the enriched group). **(B)** A comparative plot of copy number alterations between TLBCL cases and PCNSL, highlighting the biologically relevant region with differential frequency. PCNSL CNA segments with lengths below 100 kbp were filtered out for this comparison. Frequent alterations in centromeric and telomeric regions and IG loci (IGK, IGH, and IGL) were displayed but not indicated as differentially altered regions since they were not filtered out in the PCNSL series. **(C)** Comparison of gene mutation frequencies between TLBCL, DLBCL, and PCNSL. Only genes mutated in more than 7.5% of the cases are shown. TLBCL mutations with VAF<10% were filtered out when comparing the TLBCL and PCNSL series, but not in the represented frequencies. *Denote several adjusted *p*-value (Q-value) thresholds when comparing the TLBCL series to the DLBCL or the PCNSL one.

(Supporting Information S1: Figure 6). The CN complexity was not assessed considering the different resolutions of the applied technologies. 6p21.32 (*HLA-DRA*) deletion was the only alteration more prevalent in PCNSL, and no significant differences in specific genes between both groups were observed (Figure 3 and Supporting Information S1: Tables 13 and 14).

We also performed the comparative analysis considering only localized TLBCL cases with similar findings, with main driver genes like *PIM1*, *MYD88*^{L265P}, *CD79B*, *ETV6*, and *TBL1XR1* being enriched in TLBCL (Supporting Information S1: Figure 7). In addition, we also identified enrichment of *BTG1* mutations in localized TLBCL compared to nodal DLBCL, not detected in the above comparison between TLBCL (localized/disseminated) versus nodal DLBCL. Regarding the CN profile, no clear differences were observed between the groups, which could be explained by the loss of statistical power when using fewer cases for comparisons. When comparing localized TLBCL versus PCNSL, 6p21.32 deletions remained more frequent in PCNSL (10% vs. 46%, adj. $p = 0.19$) (data not shown).

Finally, despite adjusting for the COO to account for the varying frequencies of ABC/GCB between the three entities, we exclusively compared ABC TLBCL to ABC DLBCL finding a lower number of CNA and a higher number of mutated genes and mutations in ABC TLBCL versus ABC DLBCL ($p = 0.015$, $p = 0.032$, $p = 0.01$, respectively) (Supporting Information S1: Figure 5). Furthermore, *PIM1*, *MYD88*^{L265P}, *CD79B*, *BTG1*, *TBL1XR1*, and *ETV6* mutations were more prevalent in ABC TLBCL (Supporting Information S1: Figure 8). Even when comparing only localized ABC TLBCL versus ABC DLBCL, *PIM1*, *MYD88*^{L265P}, *CD79B*, *BTG1*, and *ETV6* alterations were more frequent in localized ABC TLBCL. We observed no clear differences in the CN profile between the groups, ABC TLBCL versus ABC DLBCL or localized ABC TLBCL versus ABC DLBCL. However, due to the low number of TLBCL-GCB cases ($n = 5$), we could not compare GCB TLBCL with GCB DLBCL. Nonetheless, the genomic profile of these cases is displayed in Supporting Information S1: Figure 9. Overall, regardless of the COO subtype, TLBCL localized or disseminated were enriched in *PIM1*, *MYD88*^{L265P}, *CD79B*, and *ETV6* alterations as compared to nodal DLBCL or only ABC DLBCL (Supporting Information S1: Figure 10).

Conversely, TLBCL displayed a similar genomic profile to PCNSL, except for 6p21.3 (HLA-DR) deletions, which were enriched in PCNSL.

We further applied hierarchical clustering analysis based on the genetic alterations of the cases from TLBCL, DLBCL, and PCNSL cohorts. Most TLBCL and PCNSL clustered together, whereas the majority of DLBCL grouped in a different cluster (Supporting Information S1: Figure 11). Genetic aberrations in several genes distinguished TLBCL and PCNSL from DLBCL, supporting the grouping of primary large B-cell lymphoma of the testis and CNS.

Clinical impact of initial variables and genetic lesions

After frontline treatment, 45 (80%) patients achieved complete response (CR), 1 (2%) had a partial response, and 10 (18%) were refractory, including six early deaths. Among CR patients, 13/45 (29%) eventually relapsed at a median of 26 months from achieving CR (range 3–93 months). PFS and OS at 5 years were 49% (95% confidence interval [CI]: 36–65) and 51% (95% CI: 40–69), respectively. With a median follow-up of 7 years, 29 patients (48%) had died: 13 patients due to progression, including two patients that received palliative care, and 16 due to causes other than TLBCL, including second neoplasms ($N = 4$), infection, and treatment-related toxicity ($N = 5$) and other ($N = 7$). Patients with evidence of CNS at diagnosis had a shorter PFS (HR: 3.28, 95% CI: 1.1–9.8; $p = 0.02$). Clinical variables associated with a shorter OS in the univariate analysis were high β2-microglobulin (HR: 2.99, 95% CI: 1.1–8.2; $p = 0.02$) and CNS involvement (HR: 3.32, 95% CI: 1.1–9.7; $p = 0.03$) (Supporting Information S1: Table 15). The only two mutations associated with poor PFS were *ATM* (HR: 4.1, 95% CI: 1.5–11.1; adjusted $p = 0.161$) and *SPEN* (HR: 3.8, 95% CI: 1.3–10.8; adjusted $p = 0.209$) (Supporting Information S1: Table 16).

DISCUSSION

In the present study, we analyzed the clinical and biological features of 61 cases of TLBCL treated in the rituximab era and compared the genetic profile with that previously published in nodal DLBCL and PCNSL series.[21,22] In our cohort, 30% of the patients presented with disseminated disease at diagnosis, in line with previous studies.[6,9] Although distinguishing stage III/IV TLBCL from systemic DLBCL with secondary testicular involvement is difficult and somewhat arbitrary, we did not find major differences in CNAs or mutational profiles between the two situations. In a recent study by Wong et al.,[31] few genetic differences were observed between isolated TLBCL confined to the testes and those with advanced-stage disease. They observed *CD58* truncating mutations more frequently in stages II–IV (31%; $q < 0.1$), while *BTG2* mutations were more commonly detected in stage I disease (37% vs. 8%; $q < 0.1$). Similarly, our analysis revealed an enrichment of *BTG1* mutations in localized TLBCL compared to nodal DLBCL.

We confirmed that most TLBCL have a non-GC phenotype, with only 17% classified as GCB phenotype by IHC and Lymph2Cx. This supports the rarity of TLBCL cases with a GCB subtype, as previously reported, with the ABC/non-GCB phenotype representing 69% to 96% of cases.[1,10–12] Of note, eight of the nine GCB subtype cases by Hans' algorithm had an ambiguous immunophenotype, co-expressing CD10 and MUM1, and 3 of these cases were reclassified as ABC and 1 as unclassified by Lymph2Cx. Booman et al.,[12] reported that 8 out of 22 cases of TLBCL (36%) were classified as ambiguous by IHC and were mainly reclassified as ABC subtype (7/8) using gene expression analysis. Our findings agree with those of Frauenfeld et al.[32] who described a series of DLBCL coexpressing CD10, BCL6, and MUM1. According to GEP, 32/54 (59%) cases were classified as GCB, 16/54 (30%) as ABC, and 6/54 (11%) as unclassifiable. This highlights the low correlation between Hans' algorithm and GEP profiling in cases with aberrant CD10 and MUM1 coexpression.

Using a comprehensive genomic analysis, we identified that TLBCL is characterized by alterations in genes involved in BCR activation (*CD79B*, *SGK1*), TLR signaling (*MYD88*), NF-kB (*PIM1*, *TNFAIP3*) pathway, genomic instability or cell cycle control (*CDKN2A/B*), immune evasion (*HLA-C* and *HLA-B*), B cell differentiation (*PRDM1*), and epigenetic modulators (*ARID1B*). In the recent proposed molecular classification for DLBCL, most TLBCLs cluster within the MCD/C5/MYD88 group,[13,14,33] enriched for *MYD88* and *CD79B* mutations. Using the LymphGen algorithm, the MCD group was the most frequent in our series, accounting for 66% of the cases. Alterations in $MYD88^{L265P}$ and *CD79B* are a hallmark of extranodal.[15,16] Several studies reported the high prevalence of these mutations in PCNSL, breast, and intravascular DLBCL.[15,16,22,34–39] Furthermore, additional alterations detected in TLBCL as *TNFAIP3* inactivation or *BCL2* gains have been reported to cooperate with $MYD88^{L265P}$.[40]

Mutations within genes mediating immune surveillance are key players in the TLBCL pathogenesis, including losses of the HLA class I and II loci, which are associated with reduced expression of major histocompatibility complexes (MHC).[41] In our series, we detected 6p21 (*HLA*) losses in 15% of the cases, and MHC I and MHC II loss of expression in 91% and 62% of the cases, respectively. Other studies consistently report that there are twice as many cases of TLBCL lacking MHC I and II expression compared to nodal ABC-DLBCL.[17,41] Other immune evasion mechanisms described in TLBCL are the 9p24.1 (*PD-L1*/*PD-L2*) gains or translocations and deletions/mutations of *B2M* gene on 15q21. Chapuy et al.[16] reported *PD-L1* and/or *PDL-L2* gains in half of TLBCL and *PD-L1* or *PD-L2* translocation in 4% of the cases. Nevertheless, the high prevalence of 9p24 alterations was not corroborated in a recent study,[17] neither in our cohort. In contrast, we confirmed the prevalence of 15q21 (*B2M*) deletions in TLBCL (21%, 9/43 cases), mutations in 10 cases (24%, 10/42), and concomitant deletions and mutations in 3 cases (8%, 3/40).

The genetic landscape of TLBCL shows some similarities to nodal DLBCL, but it has also distinct features. The genetic instability in TLBCL is driven by *CDKN2A/B* deletions, whereas nodal DLBCL is usually characterized by 13q14 (*RB1*) losses, 8q24 (*MYC*) gains, or *TP53* alterations.[16,42,43] A noteworthy observation was the marked occurrence of *TBL1XR1* and *MEF2B* mutations in TLBCL compared to nodal DLBCL. *TBL1XR1* mutations modify the humoral immune response by promoting memory B cells and have been linked with extranodal ABC DLBCL that originate from memory B cells.[44] Consistent with previous discoveries in PCNSL,[22] we observed a simultaneous occurrence of mutations in $MYD88^{L265P}$ and *TBL1XR* in 86% (12/14) of the cases. On the other hand, *MEF2B* deregulates the transcription of *BCL6* oncogene.[45] Lastly, *ETV6* alterations were also more prevalent in TLBCL compared to DLBCL. *ETV6* alterations have been previously detected more frequently in PCNSL than in systemic DLBCL, corroborating the similar genomic profile of both extranodal DLBCL, PCNSL, and TLBCL.[16,46,47]

TLBCL cases exhibited genomic heterogeneity, with seven out of 40 cases classified as B2N, indicating that not all TLBCL cases have the MCD genetic profile. This suggests that TLBCL is not a homogeneous disease in terms of its genetic profile. However, further cases are needed to confirm this finding.

Although previous studies pointed to some common genetic alterations between TLBCL and PCNSL, a distinguishing feature of our study is the relatively large sample size (N = 40 patients with genomic analysis) and the integration of targeted NGS and CNAs arrays, with a substantially higher number of evaluated genes (115 genes). Compared to PCNSL, TLBCL did not show major differences in CNA or mutational profile. A potential constraint of our study is that we employed targeted sequencing rather than whole-exome or whole-genome sequencing methods, which would have allowed for the assessment of genes not encompassed in our panel design.

Due to the number of cases, it was difficult to find significant correlations with prognosis in the current study. Nevertheless, it is noteworthy that patients carrying *ATM* and *SPEN* alterations had a shorter PFS. *ATM* is a well-known key regulator of the double-strand break DNA damage response pathway and cooperates with other key kinases of DNA damage. *ATM* has been described as recurrently altered in chronic lymphocytic leukemia and conventional mantle cell lymphoma, facilitating the development of structural genomic complexity of these tumors with a negative impact on the outcome of the patients.[48,49] *SPEN* alterations, a gene that encodes a hormone-inducible transcriptional repressor, have been previously described in indolent and aggressive lymphomas and associated with poor PFS.[50,51]

In conclusion, our comprehensive analysis of the mutational profile and CNAs in TLBCL revealed frequent alterations that overlap with that of another aggressive lymphoma arising in an immune-privileged site, PCNSL. Our findings demonstrated that TLBCL has a distinctive genomic signature, supporting its recognition as a separate entity from DLBCL, encouraging the grouping of primary large B-cell lymphoma of the testis and CNS, and might provide relevant information to tailor therapeutic approaches.

ACKNOWLEDGMENTS

This work was mainly developed at the Centre Esther Koplowitz (CEK), Barcelona, Spain. The authors thank the Hematopathology Collection registered at the Biobank of Hospital Clínic-IDIBAPS for sample procurement. We want to particularly acknowledge patients and Biobank HUB-ICO-IDIBELL (PT20/00 171) integrated into the Spanish Biobank Network and Xarxa Banc de Tumors de Catalunya (XBTC) for their collaboration. We are indebted to the IDIBAPS Genomics core facility. We are grateful to Sílvia Ruiz, Sílvia Martín, and Núria Russiñol for their technical and logistic assistance.

AUTHOR CONTRIBUTIONS

Alfredo Rivas-Delgado and Cristina López analyzed and interpreted data and wrote the manuscript. Guillem Clot performed statistical and clinical analyses. Ferran Nadeu performed bioinformatic analysis. Gerard Frigola, Jan Bosch-Schips, Fina Climent, and Elías Campo reviewed the H-E and immunostains. Alfredo Rivas-Delgado and Cristina López performed sample preparation and centralized clinical data. Miguel Alcoceba, Gustavo Tapia, Luis Luizaga, Carmen Barcena, Nicholas Kelleher, Neus Villamor, Tycho Baumann, Alejandro M. García-Sancho, Juan M. Sancho-Cia, Ana Muntañola, Eva Gonzalez-Barca, Estella Matutes, Jordi A. Brito, and Eva Giné, provided samples and/or clinical data. Anna Enjuanes contributed to the panel design. Kennosuke Karube and Itziar Salaverria generated and provided data from the nodal DLBCL cohort. Josefine Radke, Naveed Ishaque, Stefan Wiemann, Frank L. Heppner, and Reiner Siebert generated and provided data from the PCNSL cohort. Alfredo Rivas-Delgado, Cristina López, Marta Grau, Ferran Nadeu, Guillem Clot, Armando López-Guillermo, and Silvia Beà analyzed and interpreted data. Silvia Beà and Armando López-Guillermo designed the study, supervised the research, interpreted data, and wrote the manuscript. All authors read, commented on, and approved the manuscript.

CONFLICT OF INTEREST STATEMENT

Ferran Nadeu has received honoraria from Janssen, AbbVie, AstraZeneca, and SOPHiA GENETICS for speaking at educational activities; has received research support from Gilead; and has licensed the use of the protected IgCaller algorithm to Diagnóstica Longwood. Tycho Baumann has received consulting fees or honoraria from Janssen, Roche, Novartis, Merck, Gilead/Kite, Incyte, Lilly, Abbvie, AstraZeneca, and BeiGene. Alejandro Martin García-Sancho has

received consulting fees or honoraria from Janssen, Roche, BMS/Celgene, Kyowa Kirin, Clinigen, EUSAPharma, Novartis, Gilead/Kite, Incyte, Lilly, Takeda, ADC Therapeutics America, Miltenyi, Ideogen, Abbvie, and BeiGene. Elías Campo has been a consultant for GenMab, and Takeda; has received research support from AstraZeneca; received honoraria from Janssen, EUSPharma, Takeda, and Roche for speaking at educational activities; and is an inventor on a Lymphoma and Leukemia Molecular Profiling Project patent "Method for subtyping lymphoma subtypes by means of expression profiling" (PCT/US2014/64161) and a bioinformatic tool (IgCaller) licensed to Diagnostic Longwood. Eva Giné has received honoraria or consulting fees from Gilead, Kite Pharma, Janssen, Genmab, Miltenyi, and Lilly; has received research support from Janssen and travel expenses from Gilead and Kite Pharma. Armando López Guillermo served on the advisory board of Roche, Celgene, Novartis, and Gilead/Kite, received grants from Celgene and Gilead/Kite, and travel expenses from Kite/Gilead. The remaining authors declare no competing interests.

DATA AVAILABILITY STATEMENT

Our entire genomic data set, including next-generation sequencing (NGS) and copy number alteration (CNA) arrays, are deposited at the European Genome-phenome Archive under accession no. EGAS50000000521 (https://ega-archive.org/studies/EGAS50000000521).

FUNDING

This study was supported by Fundación Asociación Española Contra el Cancer AECC/CIBER: PROYE18020BEA (S.B.); Fondo de Investigaciones Sanitarias, Instituto de Salud Carlos III Instituto de Salud Carlos III, "Cofinanciado por la Unión Europea" and Fondos FEDER: European Regional Development Fund "Una manera de hacer Europa": PI19/00887 (A.L-G. and E.G.), PI22/00203 (S.B. and E.G.) and INT23/00037 (to S.B.), PI23/01500 (A.L-G.) and INT20/00050 (A.L-G); MCIN/AEI/10.13039/501100011033 and FEDER European Regional Development Fund "Una manera de hacer Europa": PID2021-123054OB-I00 (E.C.). Marató TV3 TV3-Cancer/201904-30 (S.B.); Generalitat de Catalunya, Suport Grups de Recerca AGAUR: 2021-SGR-01293 (S.B.), 2021-SGR-01274 (E.G.), 2021-SRG-01172 (E.C.). The ICGC MMML-seq Project was supported by the German Ministry of Science and Education (BMBF) in the framework of the ICGC MMML-Seq (01KU1002A-J) and the ICGC DE-Mining (01KU1505G and 01KU1505E). A.R-D is supported by a grant from Fundación Española de Hematología y Hemoterapia. C.L. is supported by a postdoctoral Beatriu de Pinós grant from Secretaria d'Universitats i Recerca del Departament d'Empresa i Coneixement de la Generalitat de Catalunya and by Marie Sklodowska-Curie COFUND program from H2020 (2018-BP-00055). F.N. is supported by the American Association for Cancer Research (2021 AACR-Amgen Fellowship in Clinical/Translational Cancer Research, 21-40-11-NADE), the European Hematology Association (EHA Junior Research Grant 2021, RG-202012-00245), and the Lady Tata Memorial Trust (International Award for Research in Leukaemia 2021-2022, LADY_TATA_21_3223). M.G. was funded by FPI pre-doctoral fellowship: PRE2019-088443. E.C. is an Academia Researcher of the "Institució Catalana de Recerca i Estudis Avançats" of the Generalitat de Catalunya.

ORCID

Alfredo Rivas-Delgado http://orcid.org/0000-0003-0385-3415
Silvia Beà https://orcid.org/0000-0001-7192-2385

SUPPORTING INFORMATION

Additional supporting information can be found in the online version of this article.

REFERENCES

1. Cheah CY, Wirth A, Seymour JF. Primary testicular lymphoma. *Blood*. 2014;123:486-493.
2. Møller MB, d'Amore F, Christensen BE. Testicular lymphoma: a population-based study of incidence, clinicopathological correlations and prognosis. *Eur J Cancer*. 1994;30A:1760-1764.
3. Menter T, Ernst M, Drachneris J, et al. Phenotype profiling of primary testicular diffuse large B-cell lymphomas. *Hematol Oncol*. 2014;32:72-81.
4. Alaggio R, Amador C, Anagnostopoulos I, et al. The 5th edition of the World Health Organization classification of haematolymphoid tumours: lymphoid neoplasms. *Leukemia*. 2022;36:1720-1748.
5. Campo E, Jaffe ES, Cook JR, et al. The international consensus classification of mature lymphoid neoplasms: a report from the Clinical Advisory Committee. *Blood*. 2022;140:1229-1253.
6. Gundrum JD, Mathiason MA, Moore DB, Go RS. Primary testicular diffuse large B-cell lymphoma: a population-based study on the incidence, natural history, and survival comparison with primary nodal counterpart before and after the introduction of rituximab. *J Clin Oncol*. 2009;27:5227-5232.
7. Fonseca R, Habermann TM, Colgan JP, et al. Testicular lymphoma is associated with a high incidence of extranodal recurrence. *Cancer*. 2000;88:154-161.
8. Deng L, Xu-Monette ZY, Loghavi S, et al. Primary testicular diffuse large B-cell lymphoma displays distinct clinical and biological features for treatment failure in rituximab era: a report from the International PTL Consortium. *Leukemia*. 2016;30:361-372.
9. Mazloom A, Fowler N, Medeiros LJ, Iyengar P, Horace P, Dabaja BS. Outcome of patients with diffuse large B-cell lymphoma of the testis by era of treatment: the M. D. Anderson Cancer Center experience. *Leuk Lymphoma*. 2010;51:1217-1224.
10. Li D, Xie P, Mi C. Primary testicular diffuse large B-cell lymphoma shows an activated B-cell-like phenotype. *Pathol Res Pract*. 2010;206:611-615.
11. Al-Abbadi MA, Hattab EM, Tarawneh MS, Amr SS, Orazi A, Ulbright TM. Primary testicular diffuse large B-cell lymphoma belongs to the nongerminal center B-cell-like subgroup: a study of 18 cases. *Mod Pathol*. 2006;19:1521-1527.
12. Booman M, Douwes J, Glas A, de Jong D, Schuuring E, Kluin P. Primary testicular diffuse large B-cell lymphomas have activated B-cell-like subtype characteristics. *J Pathol*. 2006;210:163-171.
13. Wright GW, Huang DW, Phelan JD, et al. A probabilistic classification tool for genetic subtypes of diffuse large B cell lymphoma with therapeutic implications. *Cancer Cell*. 2020;37:551-568.
14. Chapuy B, Stewart C, Dunford AJ, et al. Molecular subtypes of diffuse large B cell lymphoma are associated with distinct pathogenic mechanisms and outcomes. *Nat Med*. 2018;24:679-690.
15. Kraan W, Van Keimpema M, Horlings HM, et al. High prevalence of oncogenic MYD88 and CD79B mutations in primary testicular diffuse large B-cell lymphoma. *Leukemia*. 2014;28:719-720.
16. Chapuy B, Roemer MGM, Stewart C, et al. Targetable genetic features of primary testicular and primary central nervous system lymphomas. *Blood*. 2016;127:869-881.
17. Minderman M, Amir A, Kraan W, et al. Immune evasion in primary testicular and central nervous system lymphomas: HLA loss rather than 9p24.1/PD-L1/PD-L2 alterations. *Blood*. 2021;138:1194-1197.
18. Swerdlow SH, Campo E, Harris NL, et al. *WHO Classification of Tumours of Haematopoietic and Lymphoid Tissues (Revised 4th Edition)*. IARC; 2017.
19. Cheson BD, Fisher RI, Barrington SF, et al. Recommendations for initial evaluation, staging, and response assessment of hodgkin and non-hodgkin lymphoma: the Lugano classification. *J Clin Oncol*. 2014;32:3059-3067.
20. Cheson BD, Ansell S, Schwartz L, et al. Refinement of the Lugano Classification lymphoma response criteria in the era of immunomodulatory therapy. *Blood*. 2016;128:2489-2496.

21. Karube K, Enjuanes A, Dlouhy I, et al. Integrating genomic alterations in diffuse large B-cell lymphoma identifies new relevant pathways and potential therapeutic targets. *Leukemia*. 2018;32:675-684.
22. Radke J, Ishaque N, Koll R, et al. The genomic and transcriptional landscape of primary central nervous system lymphoma. *Nat Commun*. 2022;13:2558.
23. Mermel CH, Schumacher SE, Hill B, Meyerson ML, Beroukhim R, Getz G. GISTIC2.0 facilitates sensitive and confident localization of the targets of focal somatic copy-number alteration in human cancers. *Genome Biol*. 2011;12:R41.
24. Nadeu F, Delgado J, Royo C, et al. Clinical impact of clonal and subclonal TP53, SF3B1, BIRC3, NOTCH1, and ATM mutations in chronic lymphocytic leukemia. *Blood*. 2016;127:2122-2130.
25. Rivas-Delgado A, Nadeu F, Enjuanes A, et al. Mutational landscape and tumor burden assessed by cell-free DNA in diffuse large B-cell lymphoma in a population-based study. *Clin Cancer Res*. 2021;27:513-521.
26. Gaujoux R, Seoighe C. A flexible R package for nonnegative matrix factorization. *BMC Bioinformatics*. 2010;11:367.
27. Ratnaparkhe M, Hlevnjak M, Kolb T, et al. Genomic profiling of Acute lymphoblastic leukemia in ataxia telangiectasia patients reveals tight link between ATM mutations and chromothripsis. *Leukemia*. 2017;31:2048-2056.
28. Salaverria I, Martín-Garcia D, López C, et al. Detection of chromothripsis-like patterns with a custom array platform for chronic lymphocytic leukemia. *Genes Chromosom Cancer*. 2015;54:668-680.
29. Ramos-Campoy S, Puiggros A, Kamaso J, et al. TP53 abnormalities are underlying the poor outcome associated with chromothripsis in chronic lymphocytic leukemia patients with complex karyotype. *Cancers*. 2022;14:3715.
30. Parker H, Rose-Zerilli MJJ, Larrayoz M, et al. Genomic disruption of the histone methyltransferase SETD2 in chronic lymphocytic leukaemia. *Leukemia*. 2016;30:2179-2186.
31. Wong J, Collinge B, Hilton LK, et al. Genetic determinants of isolated and systemic testicular diffuse large B-cell lymphoma highlight a disease spectrum. *Blood*. 2022;140(Suppl 1):6374-6375.
32. Frauenfeld L, Castrejon-De-Anta N, Ramis-Zaldivar JE, et al. Diffuse large B-cell lymphomas in adults with aberrant coexpression of CD10, BCL6, and MUM1 are enriched in IRF4 rearrangements. *Blood Adv*. 2022;6:2361-2372.
33. Lacy SE, Barrans SL, Beer PA, et al. Targeted sequencing in DLBCL, molecular subtypes, and outcomes: a Haematological Malignancy Research Network report. *Blood*. 2020;135:1759-1771.
34. Hernández-Verdin I, Kirasic E, Wienand K, et al. Molecular and clinical diversity in primary central nervous system lymphoma. *Ann Oncol*. 2023;34:186-199.
35. Schrader AMR, Jansen PM, Willemze R, et al. High prevalence of MYD88 and CD79B mutations in intravascular large B-cell lymphoma. *Blood*. 2018;131:2086-2089.
36. Franco F, González-Rincón J, Lavernia J, et al. Mutational profile of primary breast diffuse large B-cell lymphoma. *Oncotarget*. 2017;8:102888-102897.
37. Gonzalez-Farre B, Ramis-Zaldivar JE, Castrejón De Anta N, et al. Intravascular large B-cell lymphoma genomic profile is characterized by alterations in genes regulating NF-κB and immune checkpoints. *Am J Surg Pathol*. 2023;47:202-211.
38. Cao X, Li J, Cai H, Zhang W, Duan M, Zhou D. Patients with primary breast and primary female genital tract diffuse large B cell lymphoma have a high frequency of MYD88 and CD79B mutations. *Ann Hematol*. 2017;96:1867-1871.
39. Montesinos-Rongen M, Godlewska E, Brunn A, Wiestler OD, Siebert R, Deckert M. Activating L265P mutations of the MYD88 gene are common in primary central nervous system lymphoma. *Acta Neuropathol*. 2011;122:791-792.
40. Wenzl K, Manske MK, Sarangi V, et al. Loss of TNFAIP3 enhances $MYD88_{L265P}$-driven signaling in non-Hodgkin lymphoma. *Blood Cancer J*. 2018;88:97.
41. Booman M, Douwes J, Glas AM, et al. Mechanisms and effects of loss of human leukocyte antigen class II expression in immune-privileged site-associated B-cell lymphoma. *Clin Cancer Res*. 2006;12:2698-2705.
42. Monti S, Chapuy B, Takeyama K, et al. Integrative analysis reveals an outcome-associated and targetable pattern of p53 and cell cycle deregulation in diffuse large B-cell lymphoma. *Cancer Cell*. 2012;22:359-372.
43. Hernando E, Nahlé Z, Juan G, et al. Rb inactivation promotes genomic instability by uncoupling cell cycle progression from mitotic control. *Nature*. 2004;430:797-802.
44. Venturutti L, Teater M, Zhai A, et al. TBL1XR1 mutations drive extranodal lymphoma by inducing a pro-tumorigenic memory fate. *Cell*. 2020;182:297-316.e27.
45. Ying CY, Dominguez-Sola D, Fabi M, et al. MEF2B mutations lead to deregulated expression of the oncogene BCL6 in diffuse large B cell lymphoma. *Nat Immunol*. 2013;14:1084-1092.
46. Mo SS, Geng H, Cerejo M, Wen KW, Solomon DA, Rubenstein JL. Next-generation sequencing of newly-diagnosed primary CNS lymphoma reveals alterations in BTG1, ETV6, and 6p are associated with chemoresistance and inferior progression-free survival. *Blood*. 2022;140:3516-3517.
47. Bruno A, Boisselier B, Labreche K, et al. Mutational analysis of primary central nervous system lymphoma. *Oncotarget*. 2014;5:5065-5075.
48. Nadeu F, Martin-Garcia D, Clot G, et al. Genomic and epigenomic insights into the origin, pathogenesis, and clinical behavior of mantle cell lymphoma subtypes. *Blood*. 2020;136:1419-1432.
49. Puente XS, Beà S, Valdés-Mas R, et al. Non-coding recurrent mutations in chronic lymphocytic leukaemia. *Nature*. 2015;526:519-524.
50. Lee B, Lee H, Cho J, et al. Mutational profile and clonal evolution of relapsed/refractory diffuse large B-cell lymphoma. *Front Oncol*. 2021;11:628807.
51. Bonfiglio F, Bruscaggin A, Guidetti F, et al. Genetic and phenotypic attributes of splenic marginal zone lymphoma. *Blood*. 2022;139:732-747.